

Short Communication

## Effect of the Calcareous Deposits on the Stress Corrosion Cracking Behavior of 10Ni5CrMoV High Strength Steel in Deep-Sea Environment

Hongbo Xu<sup>1,2</sup>, Lin Li<sup>2,\*</sup>, Lina Peng<sup>1</sup>, Hongyu San<sup>2</sup>, Mingshuang Wu<sup>1</sup>, Xiandong Su<sup>2</sup>

<sup>1</sup> College of Chemical Engineering, University of Science and Technology Liaoning, Anshan 114051, China.

<sup>2</sup> State Key Laboratory of Metal Material for Marine Equipment and Application, Anshan Iron and Steel Group Corporation, Anshan 114009, China.

\*E-mail: [ansteellilin@163.com](mailto:ansteellilin@163.com)

Received: 3 February 2021 / Accepted: 20 March 2021 / Published: 31 March 2021

---

The calcareous deposits' effect on the stress corrosion cracking (SCC) behavior of 10Ni5CrMoV high strength steel in a marine environment was investigated by slow strain rate tests (SSRT) and microscopic observations. The results showed that the hydrogen cracking mainly controlled the SCC mechanism of 10Ni5CrMoV high strength steel. The SCC sensitivity of both the 10Ni5CrMoV steel and steel covered with calcareous deposits increased first and then decreased with ocean depth. These were consistent with the hydrogen evolution reaction current density changes, which indicates that the marine environment influenced the susceptibility of SCC by changing the permeated hydrogen concentration. Moreover, the sensitivity of SCC decreased obviously when the steel was covered with calcareous deposits. This behavior was mainly attributed to the permeated hydrogen concentration, which was hindered by the calcareous deposits.

---

**Keywords:** Calcareous deposits; Deep-sea environment; Stress corrosion; Hydrogen cracking;

### 1. INTRODUCTION

With the exploration and development of marine resources, materials in deep-sea engineering must have better-and-better properties, especially the mechanical properties of high-speed deformation resistance and excellent corrosion resistance [1]. Steel is a commonly used structural steel in deep-sea engineering. Thus, investigating its dynamic mechanical properties and corrosion resistance is of great significance to exploiting marine resources and designing and selecting deep-sea engineering materials [2].

10Ni5CrMoV steel is a kind of low alloy high strength steel with a strength not less than 785 MPa. It is often used in the structural design of ships and the marine environment. It has the advantages of high strength, high toughness, and good welding performance. However, the high hydrostatic pressure, low temperature, and dissolved oxygen of the marine environment presents a challenge for the 10Ni5CrMoV steel [3].

An efficient and common method for enhancing the properties of these materials is cathodic protection (CP). Under CP, much more OH<sup>-</sup> ions are generated near the surface, resulting in the formation of the calcareous deposits [4]. On the one hand, the calcareous deposits were equivalent to an insulating layer, increasing the metal surface's polarization resistance. The current density and the protection potential required for cathodic protection will be changed to some extent [5-8]. In our group's previous work, the calcareous deposits' influence on the cathodic protection potential of 10Ni5CrMoV high strength steel in a deep-sea environment was investigated. It was found that both the potential of the 10Ni5CrMoV covered with calcareous deposits decreased slightly compared to the uncovered ones. Moreover, the CP potential for the unprotected high-strength steel was similar to that of the one covered with calcareous deposits [9]. On the other hand, the insulating layer could also influence the growth of pitting and permeated hydrogen concentration [10-11], and both are the critical factor induced the SCC behavior of the steel [12]. However, up to date, the calcareous deposits on the stress corrosion cracking behavior of 10Ni5CrMoV high strength steel in a marine environment are unclear.

Therefore, based on clarification of the CP potential range of the steel with the calcareous deposits and the effect of the calcareous deposits on the SCC behavior of 10Ni5CrMoV high strength steel marine environment, were investigated in the present work.

## 2. EXPERIMENTAL

### 2.1 Material and solution

The material used in this work was 10Ni5CrMoV with the following chemical composition (wt.%): C, 0.08%; Si, 0.305%; Mn, 0.55%; P, 0.008%; S, 0.004%; Cr, 0.57%; Ni, 4.60%; Mo, 0.43%; V, 0.063%; Fe, all remaining. The laboratory simulation of deep-sea environmental factors, including the temperature, dissolved oxygen (DO), hydrogen pressure (HP) and pH are shown in Table 1.

**Table 1.** Laboratory simulation of deep-sea environmental factors.

Environmental factors	Depth (m)					
	0	300	600	900	1500	1800
Temperature (°C)	25	17	7	4	4	4
DO (mg/L)	6.25	3.6	0.38	0.38	0.38	0.38
HP (MPa)	0.1	3	6	9	15	18
pH	7.5	7.5	7.5	7.5	7.5	7.5

## 2.2 Slow strain rate tests (SSRT)

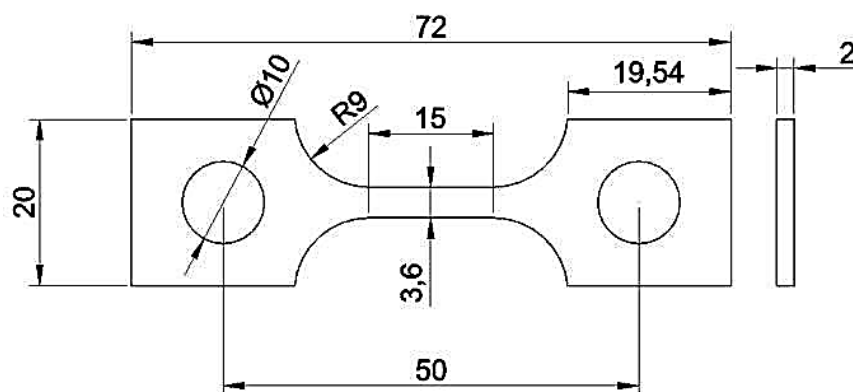


**Figure 1.** Dimensions of the SSRT test specimen (unit, mm).

The specimens for SSRT tests were prepared according to GB/T15970, as shown in Fig. 1. Before the main experiment, the specimens' gauge section was ground to 2000 grit emery paper along the tensile direction, then degreased with ethanol, washed with distilled water, and dried in air. Before starting the test, the SSRT specimens were immersed in a deep-sea environment. After immersion, the SSRT tests were performed immediately using a tensile testing system (YYF-50 kN, China), yielding a strain rate of  $10^{-6} \text{ s}^{-1}$ . Each test was reproduced three times in order to confirm the reproducibility of the results.

The SCC susceptibility of the 10Ni5CrMoV was evaluated by the elongation loss ratio ( $I_\delta$ ), reduction-in-area loss ( $I_\psi$ ) and fracture ductility loss ( $I_\epsilon$ ) according to the following equations [2]:

$$I_\delta = \left(1 - \frac{\delta_s}{\delta_0}\right) \times 100\% \quad (1)$$

$$I_\psi = \left(1 - \frac{\psi_s}{\psi_0}\right) \times 100\% \quad (2)$$

where  $\delta_s$ ,  $\delta_0$  and  $\psi_s$ ,  $\psi_0$  were the elongation and reduction-in-area of 10Ni5CrMoV.

## 2.3. Microstructure observation

The fracture surface of the 10Ni5CrMoV was cut off after removing the corrosion products, based on ASTM standard G1-03 [13]. The specimens' fracture morphologies viewed from the transverse side were observed by SEM (Quanta 200 F, USA).

# 3. RESULTS AND DISCUSSION

## 3.1. Effect of the depth of the marine environment on the SCC susceptibility

The stress-strain curves of the 10Ni5CrMoV steel specimen measured in different simulated environments are shown in Fig. 2(a). With the increase of the depth, the yield strength and tensile strength of 10Ni5CrMoV steel were enlarged first and then reduced. To investigate the factors of SCC

of the 10Ni5CrMoV steel, the elongation-loss rate ( $I_\delta$ ) and reduction-in-area loss ( $I_\psi$ ) were calculated (Fig. 2b).

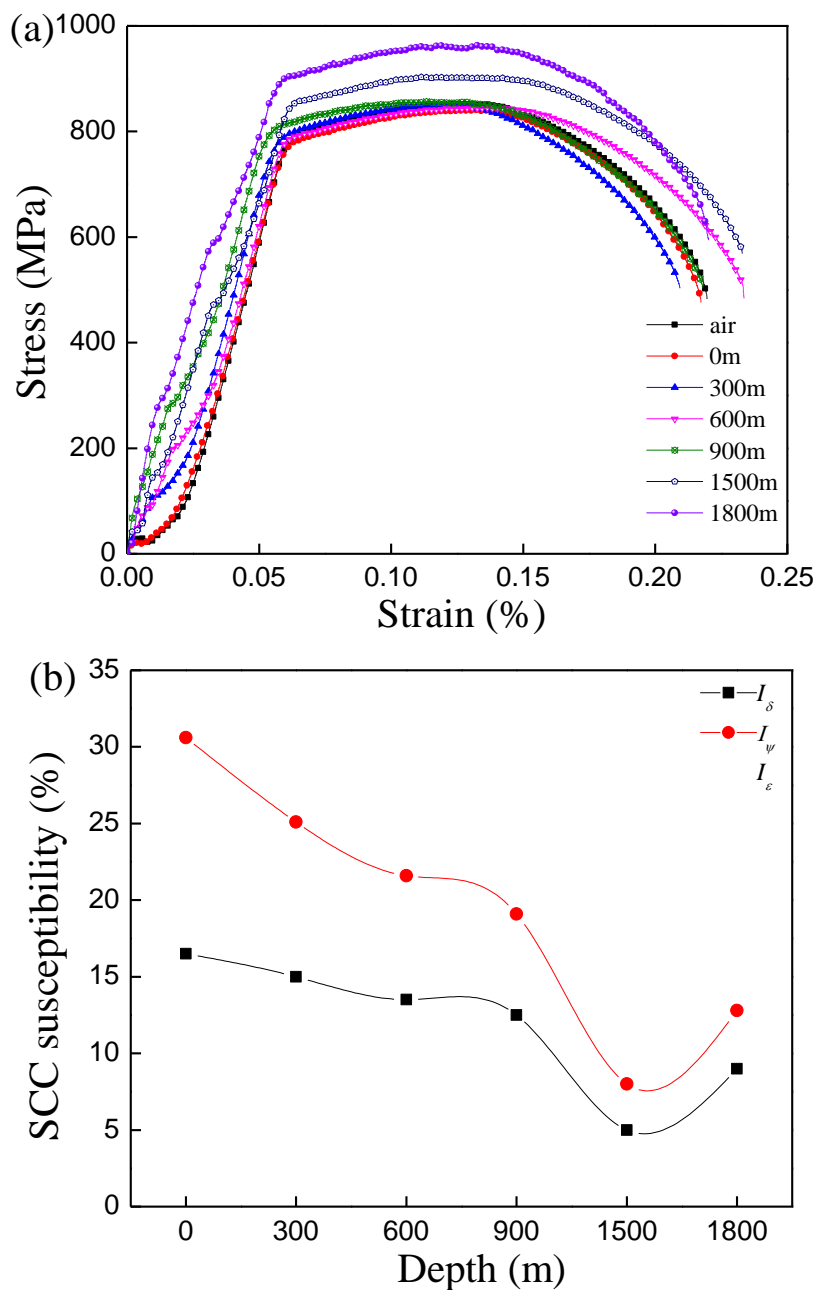


**Figure 2.** Stress-strain curves (a) and SCC susceptibilities (b) (elongation-loss rate  $I_\delta$  and reduction-in-area loss  $I_\psi$ ) of the 10Ni5CrMoV steel in the marine environment.

As shown in Fig. 2(b),  $I_\delta$  and  $I_\psi$  first decreased and then increased. The toughness loss of 10Ni5CrMoV steel was the smallest in the simulated 1500 m depth and was the largest in the simulated 0 m deep-sea environment. Similarly, 10Ni5CrMoV steel possessed the highest SCC susceptibility in the simulated 0 m deep-sea environment and the lowest in the simulated 1500 m marine environment. To investigate the SCC regularity of 10Ni5CrMoV steel, the SEM images of the cross faces of SSRT samples were examined under various conditions (Fig. 3).

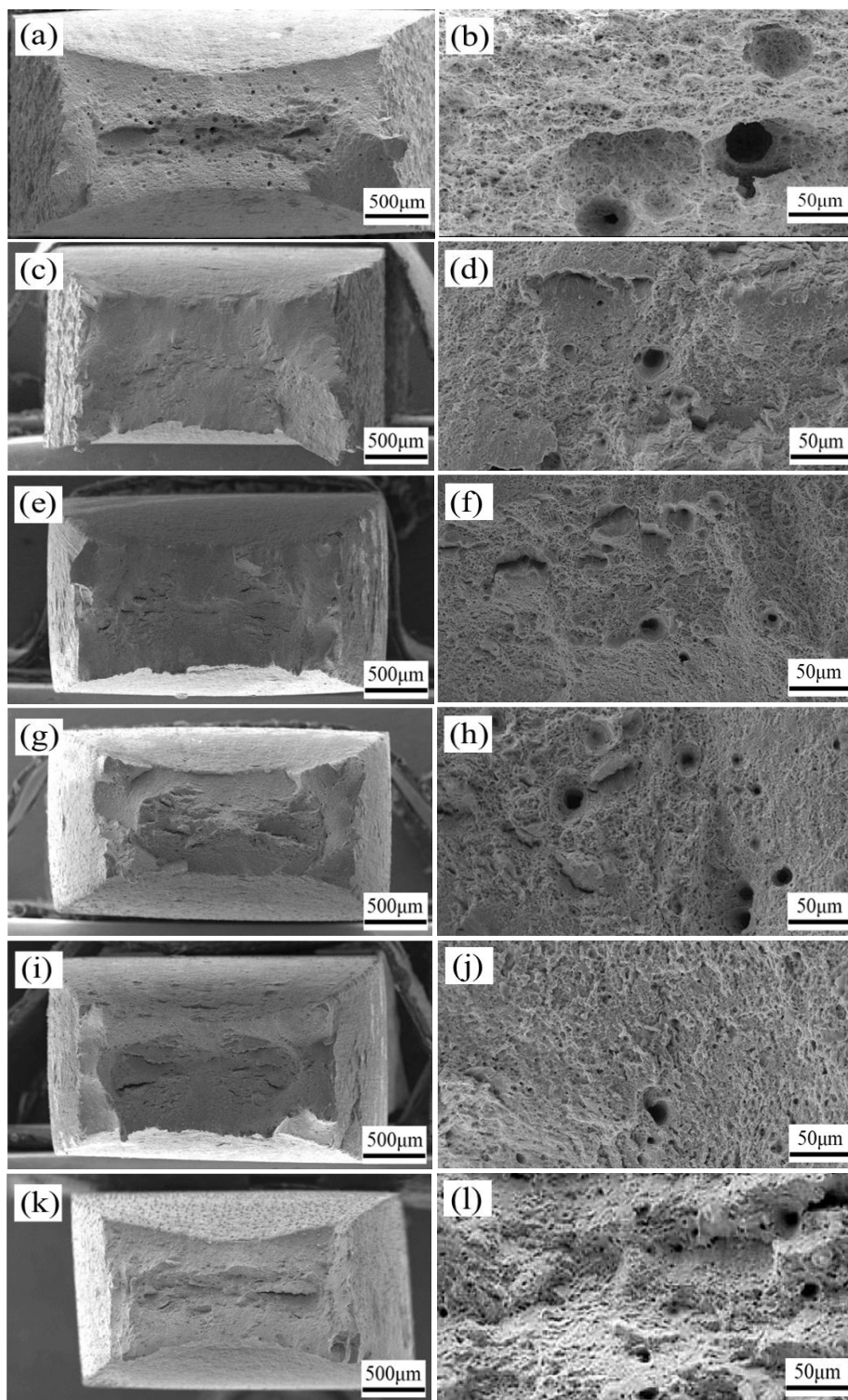


**Figure 3.** The cross morphologies of the 10Ni5CrMoV steel in different depths of the marine environment. (a)-(b) 0 m, (c)-(d) 300 m, (e)-(f) 600 m, (g)-(h) 900 m, (i)-(j) 1500 m, (k)-(l) 1800 m.

It can be observed that the fracture surfaces of specimens in the whole range of the ocean depths contained many ductile dimples, which show ductile features.

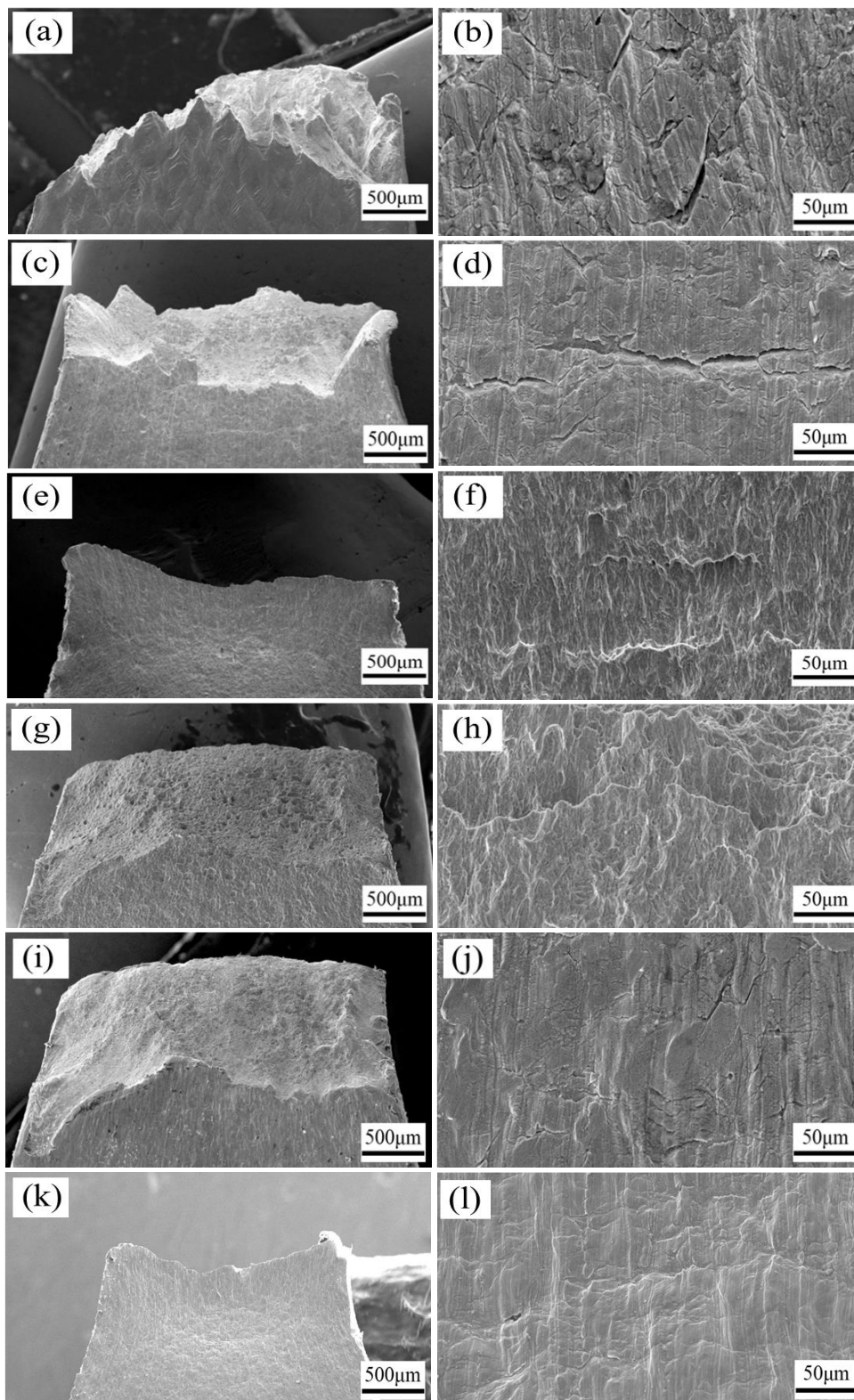


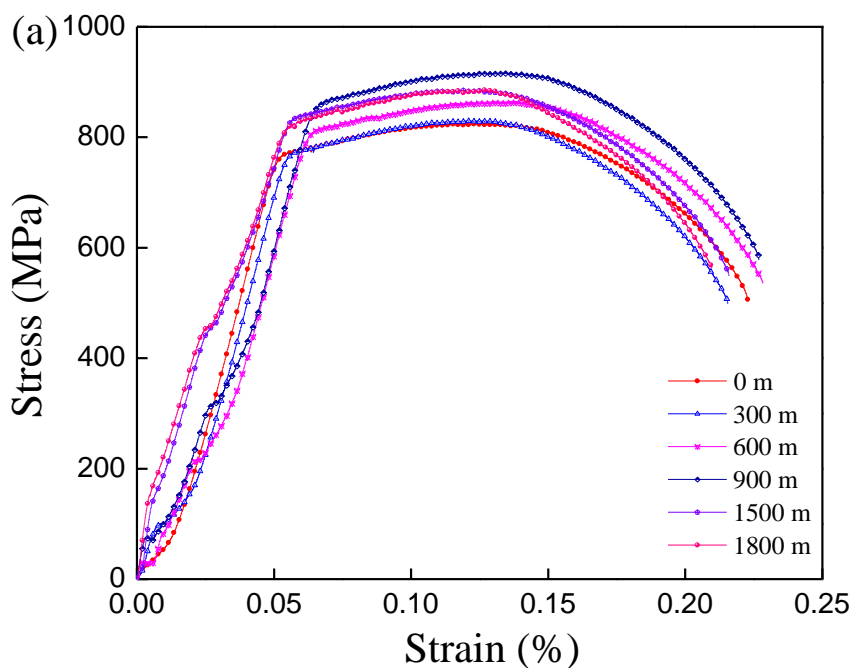
**Figure 4.** The side faces morphologies of the 10Ni5CrMoV steel in different depths of marine environment. (a)-(b) 0 m, (c)-(d) 300 m, (e)-(f) 600 m, (g)-(h) 900 m, (i)-(j) 1500 m, (k)-(l) 1800 m.

The dimples' density decreases as the depth increased to 1500 m and increased obviously as for 1800 m. Furthermore, the side faces of SSRT samples were also examined to investigate the failure

mechanisms (Fig. 4). It was observed that many micro-cracks were present on the side faces. The micro-cracks obtained in 0 m were evident, becoming smaller and larger with the increasing ocean depth. The cracks in the side face in the simulated 1500 m depth had the smallest openings. Additionally, there was no pitting corrosion, suggesting that the driving force of the SCC would result from the hydrogen [14]. The previous work [9] proved that the increased HP accelerates the cathodic hydrogen evolution reaction and inhibits the anodic reaction. Moreover, when the ocean's depth was over 1500 m, the cathodic polarization curve moved right with ocean depth. The change of hydrogen evolution reaction ( $i_H$ ) could be calculated, and the results were consistent with the rate of change of SCC susceptibility of 10Ni5CrMoV steel in simulated deep-sea environments. Generally speaking, the hydrogen accumulated at local irregularities could cause the initiation of micro-cracks [15]. Therefore, it can be concluded that the change of the SCC sensitivity of 10Ni5CrMoV high strength steel was mainly controlled by the changing of the permeated hydrogen concentration.

### 3.2. Effect of the calcareous deposits on the SCC susceptibility of the 10Ni5CrMoV steel

The stress-strain curves of the 10Ni5CrMoV steel covered by calcareous deposits are shown in Fig. 5(a). The elongation-loss rate ( $I_\delta$ ) and reduction-in-area loss ( $I_\psi$ ) were calculated (Fig. 5b). It could be observed that the SCC susceptibility of the 10Ni5CrMoV steel covered by calcareous deposits consisted of that of the bare steel.



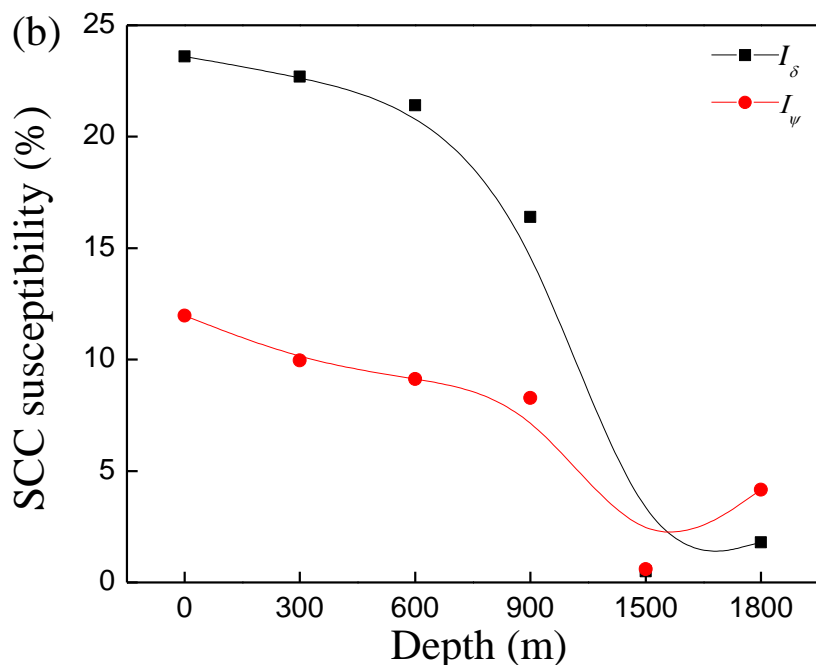


**Figure 5.** Stress-strain curves (a) and SCC susceptibilities (b) (elongation-loss rate  $I_{\delta}$  and reduction-in-area loss  $I_{\psi}$ ) of the 10Ni5CrMoV steel covered with calcareous deposits.

Moreover, the SCC sensitivity decreased obviously when the steel was covered with calcareous deposits. To investigate the sources of the reduced SCC susceptibility, the SEM images of the steel's cross and side faces were also examined (Figs. 6-7). The density of the dimples and the micro cracks in 0 m were also readily apparent, and it became smaller and then larger with the increasing depth. By contrast, all the characteristics, including the dimples and the micro-cracks, were smaller than the 10Ni5CrMoV steel uncovered by calcareous deposits. Herein, it can be assumed that the SCC sensitivity decreased when calcareous deposits covered the steel. It is well known that the calcareous deposits can behave as insulating layers, which can increase the polarization resistance of the metal surface. Thus, the  $i_H$  would also be impeded [16-17] and changed as if there were no deposits. Then the SCC susceptibility of steel covered by calcareous deposits decreased obviously. Thus, it can be concluded that the calcareous deposits had a protective effect on SCC.

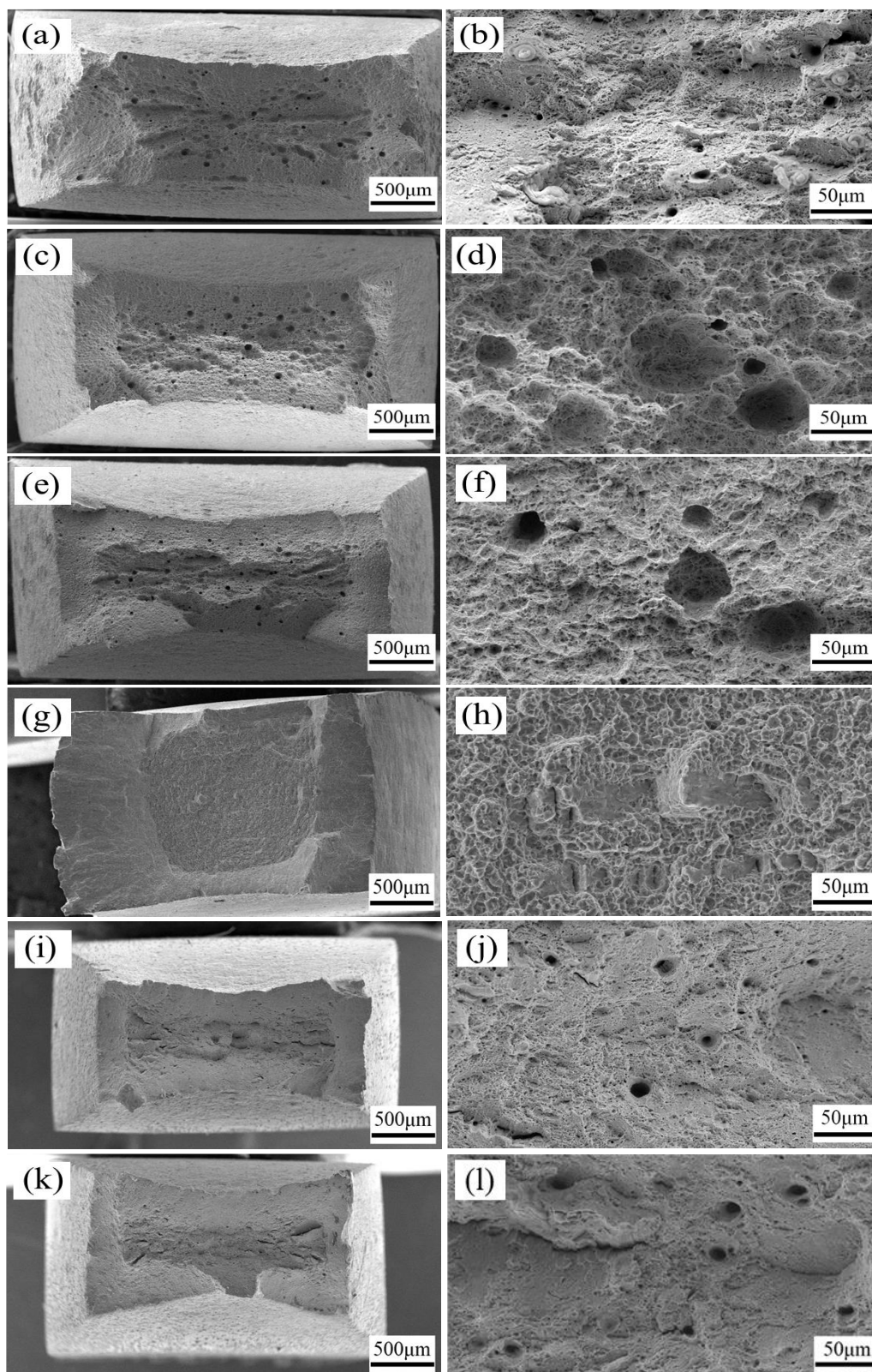


**Figure 6.** The cross morphologies of the 10Ni5CrMoV steel covered with calcareous deposits with different depths of the marine environment. (a)-(b) 0 m, (c)-(d) 300 m, (e)-(f) 600 m, (g)-(h) 900 m, (i)-(j) 15000 m, (k)-(l) 1800 m.

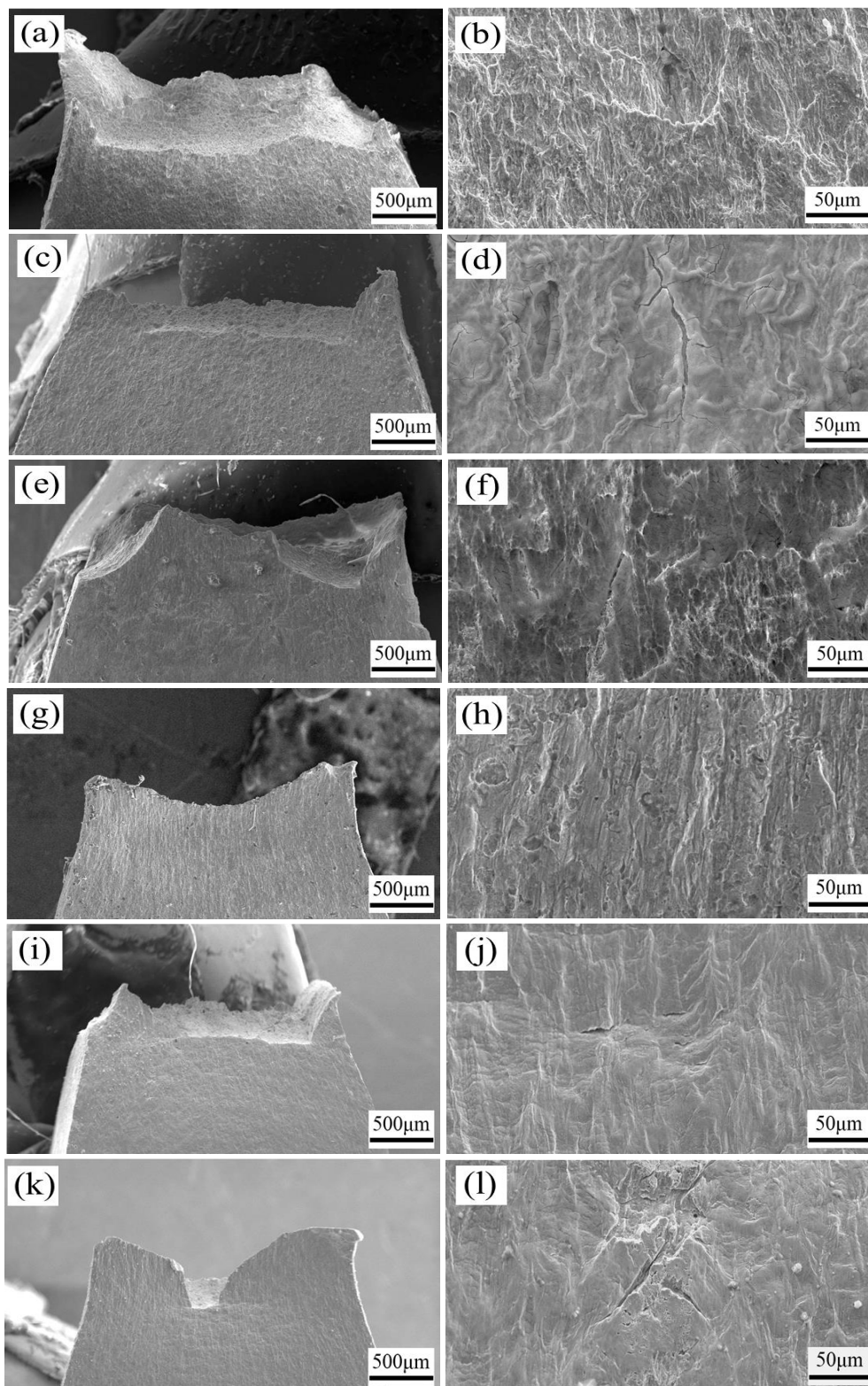


**Figure 7.** The side faces morphologies of the 10Ni5CrMoV steel covered with calcareous deposits with different depths of the marine environment. (a)-(b) 0 m, (c)-(d) 300 m, (e)-(f) 600 m, (g)-(h) 900 m, (i)-(j) 1500 m, (k)-(l) 1800 m.

#### 4. CONCLUSIONS

The SCC sensitivity of 10Ni5CrMoV high-strength steel covered with calcareous deposits decreased first and then increased with ocean depth. The hydrogen cracking mainly controlled the SCC mechanism of steel in this environment due to the changing of the permeated hydrogen concentration with the increasing depth. Moreover, the SCC sensitivity decreased obviously when the steel was covered with calcareous deposits. That was mainly attributed to the fact that the calcareous deposits impeded the permeated hydrogen concentration.

#### ACKNOWLEDGMENTS

This work was financially supported by the Joint Fund projects of University of Science and Technology Liaoning State-Key Laboratory of Metal Material for Marine Equipment and Application (No. HGSKL-USTLN(2020)04), Youth Program of National Natural Science Foundation of China (No. 52001061), Chinese Postdoctoral Science Foundation (No. 2019M651126), and National Natural Science Foundation of China (No. U1460202).

#### References

1. J. Huang, X. Liu, E. Han, X. Wu, *Corros. Sci.*, 53 (2011) 3254.
2. H. Tian, X. Wang, Z. Cui, Q. Lu, L. Wang, L. Lei, Y. Li, D. Zhang, *Corros. Sci.*, 144 (2018) 145.
3. D. Horner, B. Connolly, S. Zhou, L. Crocker, A. Turnbull, *Corros. Sci.*, 53 (2011) 3466.
4. Z. Zhang, Y. Zheng, J. Li, W. Liu, M. Liu, W. Gao, T. Shi, *Eng. Fail. Anal.*, 95 (2019) 263.
5. M. Henthorne, *Corrosion*, 72 (2016) 1488.
6. W. Mai, S. Soghrati, *Corros. Sci.*, 125 (2017) 87.
7. F. Sun, S. Ren, Z. Li, Z. Liu, X. Li, C. Du, *Mat. Sci. Eng. A*, 685 (2017) 145.
8. X. Q. Yue, M. F. Zhao, L. Zhang, H. J. Zhang, D. P. Li, M. X. Lu, *RSC Adv.*, 43 (2018) 24679.
9. H. Xu, L. Li, Y. Zhao, H. San, T. Zhang, X. Su, F. Wang, *Mater. Corros.*, 11 (2020) 1.
10. L. Calabrese, L. Bonaccorsi, M. Galeano, E. Proverbio, D. Dipietro, F. Cappuccini, *Corros. Sci.*, 98 (2015) 573.
11. X. Lei, Y. Feng, A. Fu, J. Zhang, Z. Bai, C. Yin, C. Lu, *Eng. Fail. Anal.*, 50 (2015) 62.
12. D. Spencer, M. Edwards, M. Wenman, C. Tsitsios, G. Scatigno, P. Tuckey, *Corros. Sci.*, 88 (2014) 76.
13. ASTM. Standard G1-03, *West Conshohocken*, PA, 2003.
14. R. Parkins, *Corrosion*, 52 (1996) 363-374.
15. S. Persaud, J. Smith, R. Newman, *Corrosion*, 75 (2019) 228-239.
16. Z. Cui, L. W. Wang, Z. Liu, C. W. Du, X. Li, X. Wang, *J. Mater. Eng. Perform.*, 20 (2011) 1242.
17. W. Zhao, R. Xin, Z. He, Y. Wang, *Corros. Sci.*, 63 (2012) 387-392.